Journal of Power Sources 188 (2009) 238–243

Contents lists available at ScienceDirect

Journal of Power Sources

journal homepage: www.elsevier.com/locate/jpowsour

Chemical kinetics of Ru-catalyzed ammonia borane hydrolysis

S. Basu[a,b], A. Brockman[a,b], P. Gagare[b,c], Y. Zheng[a,b,*], P.V. Ramachandran[b,c], W.N. Delgass[b,d], J.P. Gore[a,b]

[a] School of Mechanical Engineering, Purdue University, 585 Purdue Mall,, West Lafayette, IN 47907-2088, USA
[b] Energy Center in Discovery Park, Purdue University, West Lafayette, IN 47907-2022, USA
[c] Herbert C. Brown Center for Borane Research, Department of Chemistry, Purdue University, West Lafayette, IN 47907-2084, USA
[d] School of Chemical Engineering, Purdue University, West Lafayette, IN 47907-2100, USA

ARTICLE INFO

Article history:
Received 29 September 2008
Received in revised form
19 November 2008
Accepted 20 November 2008
Available online 28 November 2008

Keywords:
Hydrogen storage
Ammonia borane
Hydrolysis
Chemical kinetics

ABSTRACT

Ammonia borane (AB) is a candidate material for on-board hydrogen storage, and hydrolysis is one of the potential processes by which the hydrogen may be released. This paper presents hydrogen generation measurements from the hydrolysis of dilute AB aqueous solutions catalyzed by ruthenium supported on carbon. Reaction kinetics necessary for the design of hydrolysis reactors were derived from the measurements. The hydrolysis had reaction orders greater than zero but less than unity in the temperature range from 16 °C to 55 °C. A Langmuir–Hinshelwood kinetic model was adopted to interpret the data with parameters determined by a non-linear conjugate-gradient minimization algorithm. The ruthenium-catalyzed AB hydrolysis was found to have activation energy of 76 ± 0.1 kJ mol^{-1} and adsorption energy of -42.3 ± 0.33 kJ mol^{-1}. The observed hydrogen release rates were 843 ml H_2 min^{-1} (g catalyst)$^{-1}$ and 8327 ml H_2 min^{-1} (g catalyst)$^{-1}$ at 25 °C and 55 °C, respectively. The hydrogen release from AB catalyzed by ruthenium supported on carbon is significantly faster than that catalyzed by cobalt supported on alumina. Finally, the kinetic rate of hydrogen release by AB hydrolysis is much faster than that of hydrogen release by base-stabilized sodium borohydride hydrolysis.

1. Introduction

Energy issues and environmental concerns have generated interest in hydrogen as a transportation fuel. On-board hydrogen storage poses a challenge to the development of fuel cell powered vehicles. Chemical hydrides, such as ammonia borane (AB), are a plausible option for on-board hydrogen generation. AB is a non-toxic material that can be handled safely [1]. It has the highest material hydrogen content (about 19.6 wt.%) among all amine boranes. AB has an energy density of 2.74 kWh l^{-1}, which is higher than the energy density of 2.36 kWh l^{-1} of liquid hydrogen [2]. However, temperatures above 500 °C are required for the complete dehydrogenation of AB [2].

Dehydrogenation through AB thermolysis in its neat form [3–5] and deposited in mesoporous silica [6] have been reported in the literature. Nucleation seeding of AB through heat treatment of the material accelerates hydrogen release rate but destabilizes the solid fuel [7]. The effect of exothermic hydrogen release on stability and safety of solid AB has been reported in recent US DOE Laboratory studies [7,8]. These reports emphasize that purity is critical to thermal stability of solid AB [7,8]. It is reported [8] that 1 kg of AB, corresponding to 1.9 l of closely packed-pellets (30% void), would be required to meet the hydrogen flowrate requirements at peak vehicle load. Effective methods for regeneration of AB from the dehydrogenation products are being sought [4,9,10].

Aqueous AB is stable at room temperature [3,11,12] and its contact with catalysts can liberate hydrogen on demand. Catalytic AB hydrolysis generates three moles of hydrogen from one mole of AB consumed and the reaction can be represented as follows:

$$NH_3BH_3 + 2H_2O \xrightarrow{\text{catalyst}} NH_4^+ + BO_2^- + 3H_2 \quad (1)$$

This is an exothermic reaction with a heat of reaction of -156 kJ mol^{-1} and the products of this reaction, borate ion or boric acid, are environmentally benign [13]. Hydrogen release from AB hydrolysis in the presence of transition-metal catalysts (at 0.33 wt.% AB), non-noble metal catalysts (at 1 wt.% AB), and solid acids (at 0.33 wt.% AB) has been investigated [11–13] at room temperature in pursuit of a low-cost and efficient catalyst for the reaction. However, the kinetic parameters of these reactions have not been determined. Among the non-noble metal catalysts, 10 wt.% cobalt supported on alumina (Co/Al_2O_3) was found to be the most active catalyst [12] and among the transition-metal catalysts,

* Corresponding author at: School of Mechanical Engineering, Purdue University, 585 Purdue Mall, West Lafayette, IN 47907-2088, USA. Tel.: +1 765 494 0061; fax: +1 765 494 0530.
E-mail addresses: basu1@purdue.edu (S. Basu), acbrockm@purdue.edu (A. Brockman), pgagare@purdue.edu (P. Gagare), zhengy@purdue.edu (Y. Zheng), chandran@purdue.edu (P.V. Ramachandran), delgass@purdue.edu (W.N. Delgass), gore@purdue.edu (J.P. Gore).

0378-7753/$ – see front matter © 2008 Elsevier B.V. All rights reserved.
doi:10.1016/j.jpowsour.2008.11.085

Nomenclature

A	pre-exponential factor (mol s^{-1} (kg catalyst)$^{-1}$)
C_{AB}	concentration of NH_3BH (kmol m^{-3})
$C_{AB,0}$	initial concentration of NH_3BH_3 (kmol m^{-3})
d_p	catalyst particle diameter (μm)
E_a	activation energy (kJ mol^{-1})
ΔH_{ads}	heat of adsorption (kJ mol^{-1})
K	Langmuir adsorption equilibrium constant (m^3 $kmol^{-1}$)
K_0	Langmuir adsorption equilibrium constant at a reference temperature (m^3 $kmol^{-1}$)
k	reaction rate coefficient (kmol s^{-1} (kg catalyst)$^{-1}$)
k_n	nth-order reaction rate coefficient (kmol^{n-1} s^{-1} (kg catalyst)$^{-1}$)
m_{cat}	mass of catalyst (mg)
n	reaction order
$n_{AB,0}$	moles of ammonia borane injected into the batch reactor (mol)
n_{H_2}	moles of collected H_2 (mol)
R	universal gas constant (8.314 J mol^{-1} K^{-1})
ΔS^0	entropy change of the Langmuir adsorption isotherm (J mol^{-1} K^{-1})
T	reaction temperature (°C or K)
T_0	reference temperature (K)
T_w	wall temperature of burette (K)
t	time (s)
V_{sol}	volume of the solution (m^3)

20 wt.% platinum-on-carbon (Pt/C) produced the fastest reaction rates. It has been observed that the Pt/C catalysts are highly dispersed and show higher catalytic activity than Pt-black alone [11]. The effect of Pt catalyst on AB hydrolysis was also investigated in Ref [2]. The activation energy (E_a) of a K_2Cl_6Pt-catalyzed AB hydrolysis reaction (at 0.13 wt.% AB in D_2O) was determined to be 86.6 kJ mol^{-1} [2]. These experiments involved a temperature range of 25–35 °C. The kinetic parameters reported in Ref. [2] involve a second order dependence of the AB hydrolysis rate on the catalyst concentration in solution. However, a significantly lower activation energy E_a = 62 kJ mol^{-1} for cobalt-catalyzed AB hydrolysis (1 wt.%) has been reported for a temperature range of 20–40 °C in Ref. [12].

Recently, a preparative-scale synthesis of AB was demonstrated in Ref. [1]. The authors examined the efficiency of a series of transition-metal catalysts such as $PdCl_2$, $NiCl_2$, $CoCl_2$, and $RuCl_3$; and found $RuCl_3$ to be the most active for AB hydrolysis. They also reported liberation of ammonia from the AB hydrolysis reaction at relatively high AB concentrations (15 wt.% and 25 wt.%). Ammonia liberation was not detected at a lower (6 wt.%) concentration [1].

A complete examination of the effects of catalyst choice on the reaction rates and the appropriate reaction models and parameters was not found in the literature. Based on this, the specific objectives of the present study are to: (1) measure the intrinsic kinetics of Ru-catalyzed AB hydrolysis under isothermal conditions, after having removed the effects of internal and external diffusion, using commercially available Ru on carbon solid catalyst; the kinetics model developed in this research is also desired to interpret the kinetics measurements obtained in concentrated solutions [14]; (2) compare the effects of different catalysts on the kinetics and discuss these effects on reactor design and (3) compare the AB hydrolysis kinetics with that of sodium borohydride (SBH) hydrolysis.

The experimental methods, the kinetic models, the method for determination of the model parameters and conclusions are presented below.

2. Experimental methods

2.1. Experimental materials and conditions

Ammonia borane (purity > 98%), synthesized by a Purdue team [1], and commercial 3-wt.% Ru supported on cylindrical carbon pellets (2 mm in diameter, 3 mm in length, specific area ~1000 m^2 g^{-1}, Alfa Aesar), ground and sized prior to use, were used in the AB hydrolysis measurements. In past hydrolysis studies in this laboratory [15], this form of supported Ru catalyst was found to be more efficient than other forms, such as Ru on alumina pellets, and Ru on carbon granules. A low concentration aqueous AB solution (at 1 wt.%) and a small amount of catalyst (15.2 ± 0.1 mg) were used to limit the reaction rate to a measurable range and minimize the heat generation during the experiments.

Experiments were conducted isothermally at four temperatures: 16 °C, 25 °C, 35 °C and 55 °C. Catalyst particle size of 22.5 μm and stirring speed of 800 rpm were selected to eliminate the effects of internal and external mass diffusion. The selections of catalyst size and stirring speed are detailed in Section 2.4.

2.2. Experimental apparatus

The experimental apparatus is shown schematically in Fig. 1. A 25 ml, three-necked reaction flask was preloaded with the ground catalyst and a magnetic stirring bead. The ground catalyst was prewetted by 2 ml of deionized water to eliminate the influence of initial wetting [15]. The reaction flask was submerged in a water bath and preheated to a desired reaction temperature using a thermostatic circulator. AB (1 wt.%) solution was prepared in another flask and preheated to the desired reaction temperature by submerging into another water bath. Preheating the AB solution is desired to minimize the heating time to achieve isothermal condition [15]. Approximately 2.53 millimoles (around 7.8 ml) of the preheated AB solution were then drawn and injected into the reaction flask.

The AB solution and the ground catalyst were well mixed by using the magnetic stirrer. A hypodermic type-T (copper-constantan) thermocouple with a stainless steel sheath was used to record the temperature of the solution in reaction flask. The reaction temperature was controlled within a variation of ±0.6 °C by the thermostatic circulator. The evolving hydrogen was collected in a gas burette with a resolution of 1.0 ml. The amount of collected hydrogen in the burette was calculated using the ideal gas law with the consideration of pressure variation caused by the change of water column height. Since the mass of hydrogen gas evolved from the reactor was much smaller than the mass of the burette including the water contained, an energy balance analysis revealed that the differences between the temperatures of the collected hydrogen, the water and the burette were less than 0.1 °C. As a result, the burette outer wall temperature, T_w, was measured to represent the accumulated hydrogen gas temperature.

2.3. Experimental uncertainties

The uncertainties in the gas temperature and gas volume measurements caused ±0.7% experimental uncertainties in the mole of hydrogen collected or the mole of AB consumed. Also, random errors in time, m_{cat} and V_{sol} measurements caused ±1.83% experimental uncertainty (with 95% confidence) based upon four repeated tests under same conditions. As a result, the overall experimental uncertainties in the mole of hydrogen collected or the mole of AB consumed were estimated to be ±2.0% with 95% confidence.

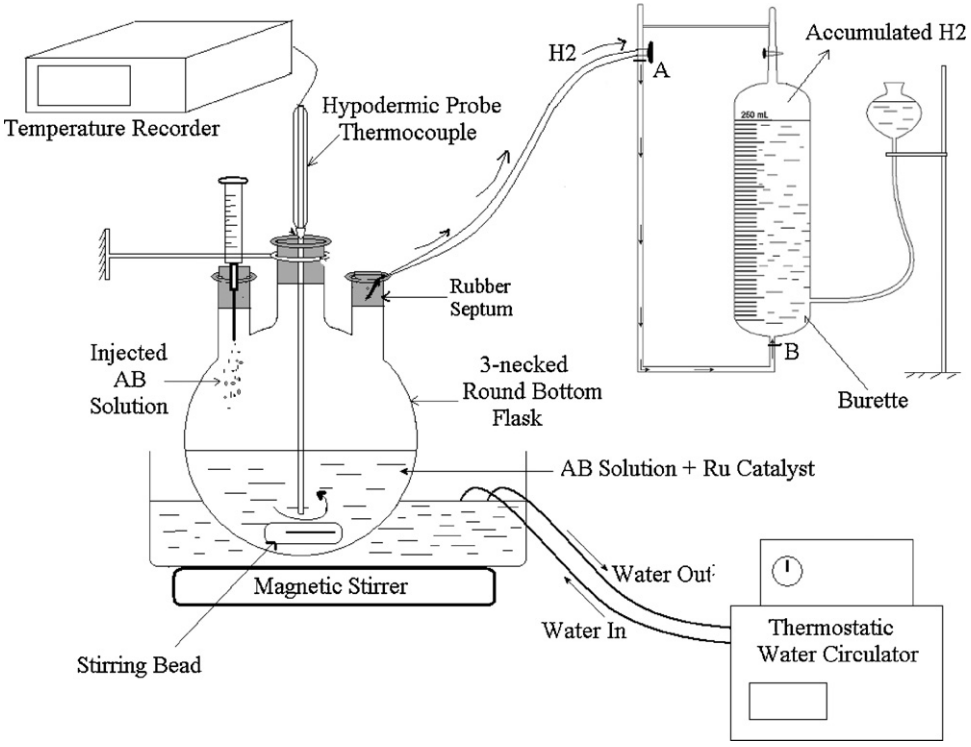

Fig. 1. Experimental apparatus.

2.4. Selections of catalyst particle size and stirring speed

To eliminate the internal mass diffusion effects, AB hydrolysis using different catalyst particle sizes was studied at the four experimental temperatures. The catalyst particles were ground and sieved into different size ranges. The sieve numbers and the average catalyst particle sizes (d_p) trapped between successive sieves are presented in Table 1. At each temperature, the catalyst particle size for which the measured reaction rates were independent of the particle size was found. The lowest particle size of 22.5 μm, at which the reaction rates were found to be free from internal mass diffusion effects at all four experimental temperatures, was used to obtain kinetic data.

In order to determine a suitable stirring speed where the hydrolysis reaction would be free from external mass diffusion, tests were conducted at 25 °C and 55 °C with stirring speeds in a range of 0 rpm to 1000 rpm. The fastest reaction rates were observed at a stirring speed of 800 rpm. The experiments at 25 °C are shown in Fig. 2. The rates observed at 1000 rpm were lower than those at 800 rpm. We assume that the mass transfer rate to the surface of the catalyst decreases as a result of reduced relative velocity between the liquid and the catalyst particles caused by entrainment at the highest stirrer speed. The optimum speed of 800 rpm was selected to obtain kinetic data that are free from external mass transfer effects.

3. Kinetic models

3.1. nth-order kinetics

For a batch reactor with a volume V_{sol} and a catalyst mass m_{cat}, the reaction order n ($n \neq 1$) can be determined using the following equation if a plot of $(C_{AB,0}^{1-n} - C_{AB}^{1-n})/(1-n)$ as a function of time gives a straight line through the origin [15]

$$\frac{C_{AB,0}^{1-n} - C_{AB}^{1-n}}{1-n} = \left(\frac{m_{cat} k_n}{V_{sol}}\right) t \quad (2)$$

where $C_{AB,0}$ is the AB concentration before hydrolysis and C_{AB} is the instantaneous AB concentration during the reaction.

3.2. Langmuir–Hinshelwood model

For a liquid phase reaction on a catalyst surface with a reaction order between zero and one, a Langmuir–Hinshelwood (LH) model can be adopted to account for the two important steps: (a) equilibrated adsorption of AB molecules on the surface of the catalyst, and (b) reaction of the adsorbed species to form hydrogen. Following Zhang et al. [15], the reaction rate can be expressed as

$$\frac{dC_{AB}}{dt} = -\frac{m_{cat}}{V_{sol}} k \frac{KC_{AB}}{1 + KC_{AB}} \quad (3)$$

where k is the reaction rate coefficient and K is the adsorption equilibrium constant. The reaction rate coefficient can be expressed as

$$k = A \exp\left(-\frac{E_a}{RT}\right) \quad (4)$$

And the adsorption equilibrium constant can be expressed as

$$K = K_0 \exp\left(\frac{\Delta H_{ads}}{RT_0} - \frac{\Delta H_{ads}}{RT}\right) \quad (5)$$

where $T_0 = 298$ K is the reference temperature.

Eq. (3) represents a zero order reaction when KC_{AB} is much greater than unity and represents a first order reaction when KC_{AB}

Table 1
Mesh ranges and pore sizes of the sieves used.

Mesh range	Range of catalyst size (μm)	d_p (μm)
#200–#230	63–75	69
#325–#400	38–45	41.5
#400–#450	32–38	35
#450–#500	25–32	28.5
#500–#635	20–25	22.5

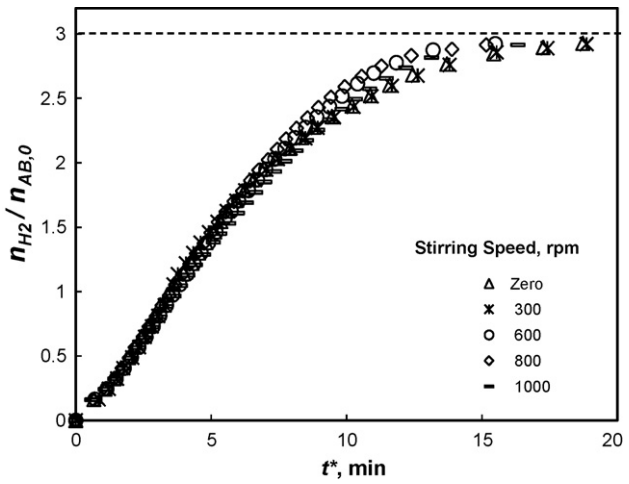

Fig. 2. Effect of stirring speed on hydrolysis rate at 25 °C, the time axis is scaled, as $t^* = ((m_{cat}/m^*_{cat})(n^*_{AB,0}/n_{AB,0}))t$, to account for differences in the catalyst masses and moles of AB injected in each of the experiments. $\left(n^*_{AB,0}, m^*_{cat}\right)$ are chosen reference values of $n_{AB,0}$ and m_{cat} in any one of the experiments.

is much less than unity. Eq. (3) also indicates that the reaction rate (dC_{AB}/dt) is proportional to m_{cat} and inversely proportional to V_{sol} at the initial part of the reaction when KC_{AB} is much greater than unity. These relationships were verified with a range of m_{cat} and V_{sol} in preliminary experiments. With all other reaction conditions same, AB was hydrolyzed at 25 °C with m_{cat} of 7.4 mg (A), 15.2 mg (B) and 29.4 mg (C) or with the ratio of 1.0:2.1:4.0. Fig. 3 presents the change of ($C_{AB,0}$–C_{AB}) with reaction time, the observed rates of reactions A, B, and C had a ratio of 1:2.1:3.8. Also, with all other reaction conditions same, AB was hydrolyzed with V_{sol} of 3.92 ml (A), 7.79 ml (B) and 12.75 ml (C) or with the ratio of 1.0:2.0:3.2. As illustrated in Fig. 4, the observed rates of reactions A, B, and C had a ratio of 1:(1/2.0):(1/2.9).

4. Determination of Langmuir–Hinshelwood kinetics model parameters

A non-linear approach was adopted to determine the four kinetics parameters, A, E_a, K_0, and ΔH_{ads}. With the assumption of zero order reaction (infinite K) in Eq. (3), ($C_{AB,0} - C_{AB}$) is a linear function of t and the slopes of these straight lines at four experimental temperatures provided the initial guess values of k. Then, an Euler predictor–corrector finite difference scheme based on Eq. (3) was used to predict the change of AB concentrations at various time steps at four temperatures as follows:

$$C_{i+1}^{\text{predicted}} = C_i - \frac{m_{cat}}{V_{sol}} k \frac{KC_i}{1+KC_i}\Delta t$$
$$C_{i+1}^{\text{corrected}} = C_i - \frac{m_{cat}}{2V_{sol}} k \left(\frac{KC_i}{1+KC_i} + \frac{KC_{i+1}^{\text{predicted}}}{1+KC_{i+1}^{\text{predicted}}}\right)\Delta t \quad (6)$$

Error minimization algorithms were then used to estimate K_0 and ΔH_{ads} simultaneously by comparing the measured and predicted change of AB concentrations. Following Powell's conjugate-gradient algorithm in conjunction with Brent's line minimization algorithm [16], K_0 and ΔH_{ads} were estimated simultaneously as a vector $\vec{Y}$ with initial guesses, for example ($2.5\ m^3\ kmol^{-1}$, $-44\ kJ\ mol^{-1}$), and two minimization directions $\vec{U}_1$ ($0.1\ m^3\ kmol^{-1}$, 0) and $\vec{U}_2$ (0, $1\ kJ\ mol^{-1}$). After updating K with the estimated K_0 and ΔH_{ads}, the k values at the four different temperatures were further refined by minimizing the differences between

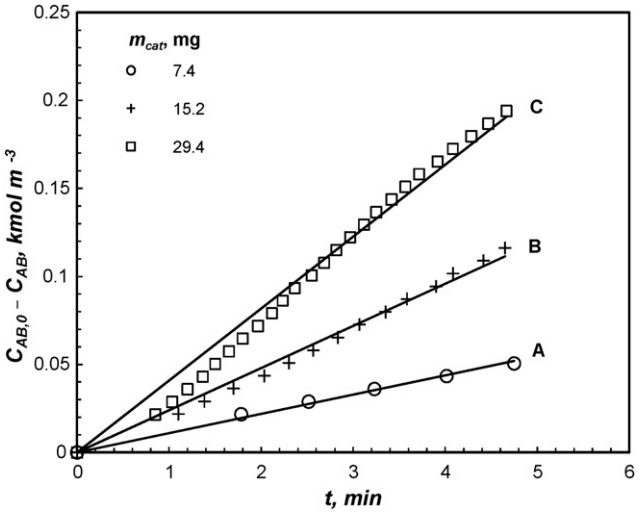

Fig. 3. Effect of catalyst mass on hydrolysis rate.

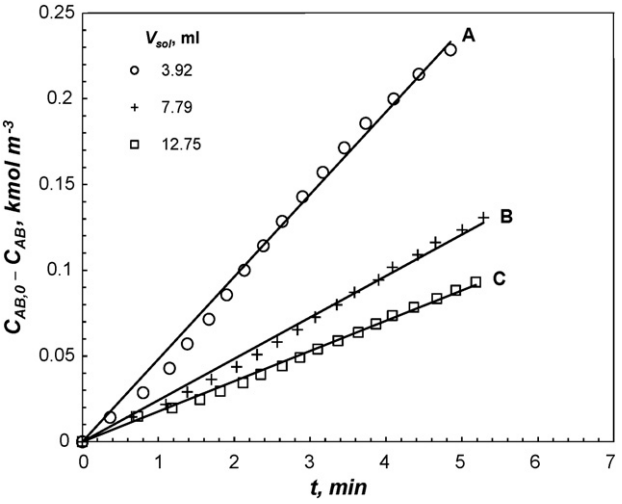

Fig. 4. Effect of solution volume on hydrolysis rate.

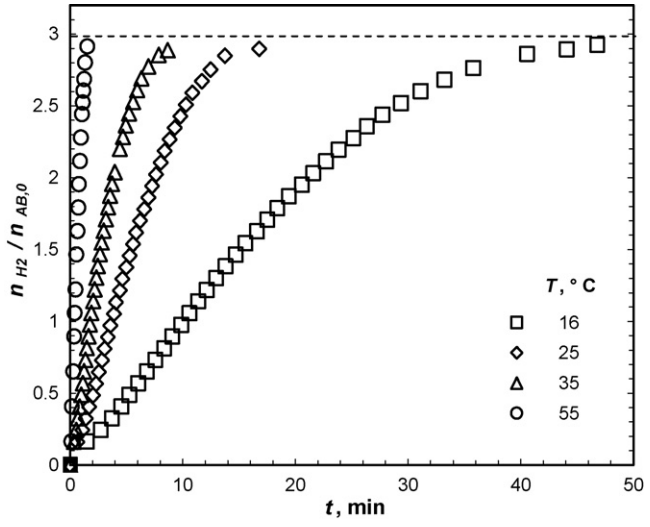

Fig. 5. Aqueous AB hydrolysis at four temperatures. Reaction conditions: V_{sol} = 9.7 ml, $n_{AB,0}$ = 2.53 mmol, m_{cat} = 15.2 mg.

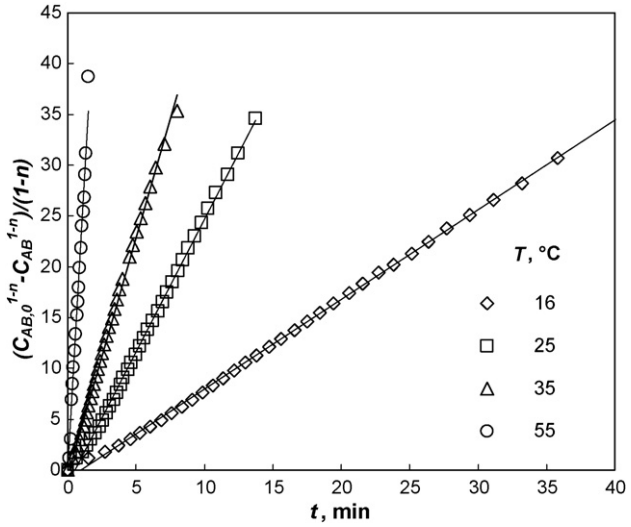

Fig. 6. Reaction orders (n) of Ru-catalyzed AB hydrolysis at four temperatures.

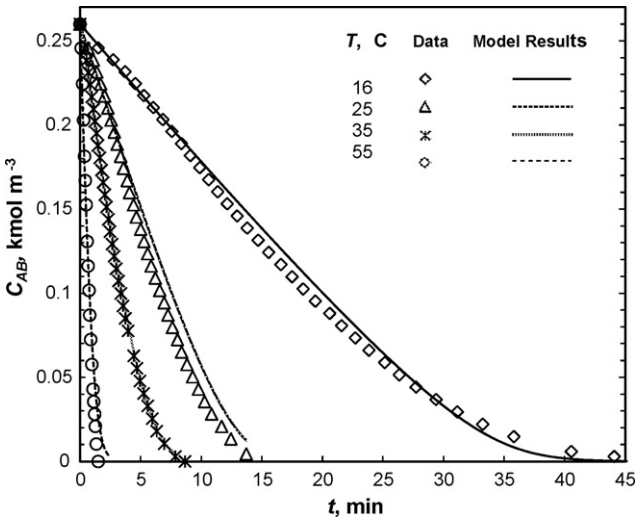

Fig. 8. Comparisons of measured and predicted AB concentration changes at four temperatures.

the predictions and measurements. Finally, A and E_a were obtained from the Arrhenius plot using updated k values. This procedure was repeated until the change in K_0 was less than 0.1 m^3 kmol^{-1} and the change in ΔH_{ads} was less than 0.5 kJ mol^{-1}. It was verified that the final results were independent of the initial guess values. The uncertainties (bounded limits) in the kinetics parameters were estimated by varying the measured C_{AB} data by ±2.0%.

5. Results and discussion

The measured moles of hydrogen evolved per mole of injected AB ($n_{H_2}/n_{AB,0}$) are presented in Fig. 5. As expected, three moles of hydrogen were generated for one mole of AB consumed at the end of the reaction. Also, the reaction rate increases rapidly with increasing temperature. Around 25 °C, the hydrogen release rate from AB hydrolysis using 3 wt.% Ru–C is 843 ml H_2 min^{-1} (g catalyst)$^{-1}$. This rate is 13× faster than that of AB hydrolysis using 10 wt.% Co-Al_2O_3, which is 63 ml H_2 min^{-1} (g catalyst)$^{-1}$ [12]. Although the cost of cobalt is much less than that of ruthenium, an on-board AB hydrolysis reactor using cobalt will be much bigger and therefore heavier than the one using ruthenium to provide the same desired hydrogen flow rate. Considering the importance of reducing weight and volume of an on-board hydrogen storage system, a tradeoff between the reactor size and cost should be considered and the final choice of the catalyst should involve an optimization of these two aspects.

It is also found that the Ru-catalyzed AB hydrolysis reaction had an average order of 0.45 in AB in the temperature range of 16–55 °C. Different guess values of n were tried until linear relationships between $(C_{AB,0}^{1-n} - C_{AB}^{1-n})/(1-n)$ and t were achieved as shown in Fig. 6.

The estimated parameters for the LH kinetics model are: $K_0 = 30.4 \pm 5.6$ m^3 kmol^{-1}, $\Delta H_{ads} = -42.3 \pm 0.33$ kJ mol^{-1}, $A = 5 \pm 0.25 \times 10^{12}$ mol s^{-1} (kg catalyst)$^{-1}$, and $E_a = 76 \pm 0.1$ kJ mol^{-1}. The Arrhenius plot, that was used to determine A and E_a using the optimized k values at the four experimental temperatures, is shown in Fig. 7. The predicted changes of AB concentrations with time at the four temperatures, using Eq. (3) and the estimated parameters, are depicted in Fig. 8. Excellent matches were achieved at 16 °C and 35 °C while slight differences exist at 25 °C and 55 °C. The overall root mean square error is 3.9% of the initial concentration of the AB solution.

We note that the average order of 0.45 used in Fig. 6 is consistent with the LH parameters but overlooks the change in order

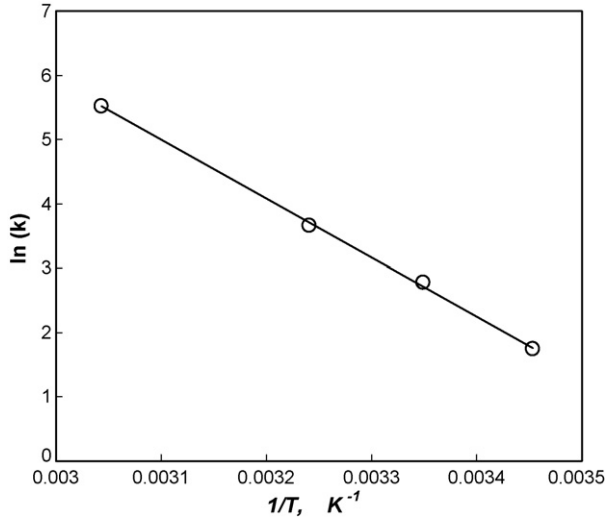

Fig. 7. Arrhenius plot using converged reaction rate coefficients at four temperatures.

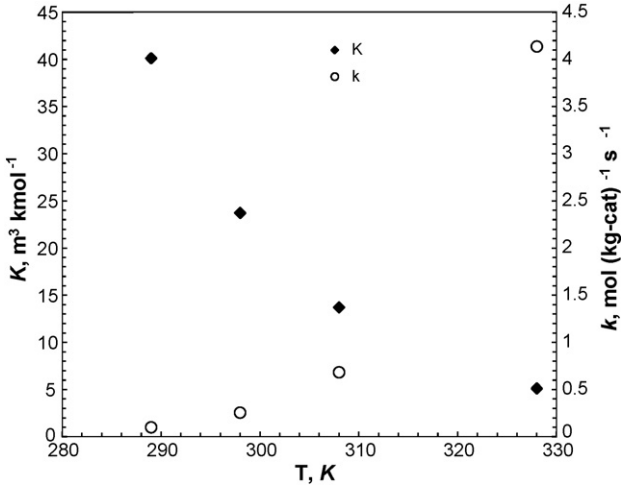

Fig. 9. Changes of reaction rate coefficients and adsorption equilibrium constants with temperature.

Table 2
Reaction properties of NH_3BH_3 and $NaBH_4$.

	AB	SBH [15]
E_a (kJ mol^{-1})	76	66.9
A (mol s^{-1} (kg catalyst)$^{-1}$)	5×10^{12}	2.19×10^{10}
k at 25 °C (mol s^{-1} (kg catalyst)$^{-1}$)	0.25	0.042
ΔH_{ads} (kJ mol^{-1})	−42.3	−35
ΔS^0 (J mol^{-1} K^{-1})	−141.8	−130
K at 25 °C (m^3 kmol^{-1})	30.4	220

expected over the wide range of composition at each temperature and from one temperature to another. We regard to LH model as a more complete description of the kinetic behavior of this system.

The reaction rate coefficients and adsorption equilibrium constants at different temperatures are depicted in Fig. 9. The adsorption equilibrium constant decreases with the increasing temperature moderately indicating stronger adsorption at low temperatures. The reaction rate coefficient, however, increases with the temperature rapidly. As a result, the reaction rate coefficient has a much stronger influence on the overall reaction rate than the adsorption equilibrium constant.

Also, the change in entropy at 25 °C of the adsorption phenomenon was calculated as follows:

$$\Delta S^0 = \frac{\Delta H_{ads}}{T_0} = \frac{-42,300 \pm 330 \ (\mathrm{J\,mol^{-1}})}{298.15 \ (K)} = -141.8 \pm 1.1 \ \mathrm{J\,mol^{-1}\,K^{-1}} \quad (7)$$

The negative value of entropy change reflects the fact that the degree of randomness decreases in an adsorption process, as expected.

Using the same 3 wt.% Ru–C, SBH hydrolysis kinetics was previously investigated [15]. The aqueous SBH solution was stabilized by adding NaOH. Base-stabilized aqueous SBH solution had a pH value of 14 which is higher than that of the aqueous AB solution (9.1 [13]). At 25 °C, there was an induction time observed in SBH hydrolysis [15] and the observed hydrogen evolution rates are 134 ml H_2 min^{-1} (g catalyst)$^{-1}$ and 843 ml H_2 min^{-1} (g catalyst)$^{-1}$ for SBH and AB hydrolysis, respectively. At 55 °C, the observed hydrogen release rates are 2047 ml H_2 min^{-1} (g catalyst)$^{-1}$ and 8327 ml H_2 min^{-1} (g catalyst)$^{-1}$ for SBH and AB hydrolysis, respectively. AB hydrolysis has much faster kinetics than SBH hydrolysis; so a packed-bed AB hydrolysis reactor would be much smaller and lighter than a SBH hydrolysis rector to provide identical hydrogen flow rates.

The reaction properties of AB and SBH hydrolysis are compared in Table 2. The higher value of K, at 25 °C, implies a lower reaction order in case of SBH hydrolysis than that of AB hydrolysis at room temperature. Also, higher E_a and ΔH_{ads} of AB hydrolysis indicate stronger temperature dependences in both reaction (k) and adsorption (K) processes than for SBH hydrolysis.

6. Conclusions

The following conclusions are drawn from the present work:

1. A non-linear fitting approach based on Powell's conjugate-gradient algorithm, developed in this study, was successful in obtaining reaction rate constants with the Langmuir–Hinshelwood (LH) model.
2. Ruthenium on carbon (Ru/C) is a suitable catalyst for the ammonia borane hydrolysis reaction. After normalizing for metallic catalyst mass, the hydrogen release rate of AB hydrolysis is 13× faster when using Ru/C catalyst than cobalt catalyst at 25 °C. The effects of the relative rates and relative costs of these catalysts on the cost of ownership need to be investigated.
3. For similar reaction conditions and a lower basicity (pH), hydrogen generation from AB is 4× and 6× faster than hydrogen generation from sodium borohydride at 25 °C and 55 °C, respectively.

Acknowledgements

This research was supported by the US Department of Energy under the contract Number DE-FC36-06GO86050 with David Peterson and Jim Alkire serving as Project Officers and Carole Read and Grace Ordaz serving as Technology Managers. This work represents a part of Sumit Basu's doctoral dissertation at Purdue University.

References

[1] P.V. Ramachandran, P.D. Gagare, Inorg. Chem. 46 (2007) 7810–7817.
[2] N. Mohajeri, A. T-Raissi, O. Adebiyi, J. Power Sources 167 (2007) 482–485.
[3] A. T-Raissi, Thermoeconomic analysis of area II, hydrogen production — Part II, Proceedings of the 2002 U.S. DOE Hydrogen Program Review, NREL/CP-610-32405.
[4] G. Wolf, J. Baumann, F. Baitalow, F.P. Hoffmann, Thermochim. Acta 343 (2000) 19–25.
[5] J. Baumann, F. Baitalow, G. Wolf, Thermochim. Acta 430 (2005) 9–14.
[6] A. Gutowska, L. Li, Y. Shin, C.M. Wang, X.S. Li, J.C. Linehan, R.S. Smith, B.D. Kay, B. Schmid, W. Shaw, M. Gutowski, T. Autrey, Angew. Chem. Int. 44 (2005) 3578–3582.
[7] C. Aardahl, T. Autrey, J. Linehan, D. Camaioni, S. Rassat, D. Rector, W. Shaw, PNNL Progress within the DoE Center of Excellence for Chemical Hydrogen Storage, http://www.hydrogen.energy.gov/pdfs/progress06/iv_b_4b_aardahl.pdf, 2006.
[8] R. Kumar, L. Verduzco, Hydrogen Storage Systems Analysis Working Group Meeting Summary Report, http://www1.eere.energy.gov/hydrogenandfuelcells/pdfs/ssawg_minutes_1206.pdf, 2006.
[9] S. Hausdorf, F. Baitalow, G. Wolf, F.O.R.L. Mertens, Int. J. Hydrogen Energy 33 (2008) 608–614.
[10] N. Mohajeri, A. T-Raissi, CIMTEC 3rd International Conference, http://www.mrs.org/s_mrs/sec_subscribe.asp?CID=2758&DID=155547&action=detail, 2008.
[11] M. Chandra, Q. Xu, J. Power Sources 156 (2006) 190–194.
[12] Q. Xu, M. Chandra, J. Power Sources 163 (2006) 364–370.
[13] M. Chandra, Q. Xu, J. Power Sources 159 (2006) 855–860.
[14] A.C. Brockman, Ammonia borane hydrolysis based hydrogen storage: engineering considerations, M.S. Thesis, Purdue University, West Lafayette, May 2008.
[15] J.S. Zhang, W.N. Delgass, T.S. Fisher, J.P. Gore, J. Power Sources 164 (2007) 772–781.
[16] R.P. Brent, Algorithms for Minimization without Derivatives, Dover Publications, Mineola, New York, 2002.